TDR Monitoring for Integrity of Structural Systems

By Miau-Bin Su[1] and Yuh-Jyh Chen[2]

Abstract: Most infrastructures are made up of large number of parts, such as truss members and bridge decks. Relative movement of the connections between members causes load redistribution or even failure. Monitoring the integrity of the structural system can assure its performance and safety. TDR (time domain reflectometry) is proposed here as a multiple-points smart monitoring system using only one coaxial cable as the sensing and conducting medium all the way through the monitored structure. The cable is fixed at both ends of each pair of adjacent members to be the sensing device along itself. Relative movements between the members at the connecting points are monitored simultaneously by sending a fast-rise impulse into the cable. When lateral movement occurs, the cable will deform, having the effect of adding an equivalent capacitance at that point and causing the signature to jump up. When two adjacent blocks move apart from each other, the cable will be extended and cause its characteristic impedance change. The most important ability for a TDR system to have is to locate the relative movement along the cable that is very clearly shown in the time domain signature. The pulse of a TDR tester can go a few thousand feet, which gives enough monitoring range for most infrastructure.

INTRODUCTION

Time domain reflectometry (TDR) was developed by electrical engineers as a method for locating discontinuities in coaxial transmission cables (Moffit 1964). The technique has been extended to measure the properties of materials in which conductors are embedded, for example, to determine soil water content (Topp et al. 1980) and evaluate the dielectric behavior of a material (Cole 1975). In rock mechanics, the technique has been employed to identify zones of rock mass deformation (Dowding et al. 1988) and blasting performance.

This technique can be applied to monitor fracturing within concrete structures (Su 1990). When a coaxial cable is embedded in a concrete structure, it works like a continuous sensor, which can detect fracture and relative movement at any location along its length. An electromagnetic pulse is launched down the cable, and reflection from points of cable deformation can be located precisely. TDR fracture monitoring provides a viable tool when fracture locations are not known in advance and is the major advantage for TDR, compared with other monitoring systems. Telemetric monitoring based on TDR theories has been proven to be applicable (Dowding and Huang 1994). Smart systems for monitoring the integrity of infrastructures are made possible by using the TDR system and techniques developed for analysis. Lin et al. (1997, 1998) discussed the concept of using TDR cable as distributed sensors in structures, but the effect of multiple reflection caused difficulty in analyzing the reflected TDR signature. Su and Chen (1998) proposed a procedure to overcome the problem. This paper presents validation tests with data from a real application.

RELATIVE MOVEMENTS BETWEEN ELEMENTS

Relative movements between concrete blocks can be divided into two categories: shear movement and normal movement. Shearing occurs when two adjacent blocks move parallel to the interface between them, and normal movement occurs when two blocks move perpendicular to the interface. Idealized pictures of block movement and associated cable deformation are shown in Fig. 1. The blocks can deform the cable by shearing [Fig. 1(b)] or extension [Fig. 1(c)].

The monitoring system for the integrity of infrastructures proposed here monitors the connection between blocks. As shown in Fig. 2, coaxial cable is fixed on two sides of a joint or a bearing point. The TDR technique can monitor many points on one coaxial cable simultaneously (Dowding et al. 1988). If two adjacent blocks move relative to one another, as shown in Figs. 1(b) and 1(c), the distorted cable no longer has a uniform cross section. The change in cable geometry causes the local cable capacitance, which is inversely proportional to the square of the distance between the outer and inner conductors, to increase or decrease. By determining the characteristic of a single shear displacement or single extension displacement under controlled laboratory conditions, it has been possible to interpret the results to estimate the magnitude of the relative shear or normal movement of the adjacent concrete blocks in which a coaxial cable has been fixed or embedded.

BASIC TDR

A coaxial cable is composed of an outer and an inner conductor with plastic dielectric material between them. In the longitudinal view, the coaxial cable may be presented as an ideal, two-wire transmission line having forward and return conductors to represent the outer and inner conductors, respectively. Propagation of a pulse along a coaxial cable, that is, the current and voltage propagating along a two-wire transmission line, is controlled by four basic properties of coaxial cables, namely, inductance, resistance, capacitance, and dielectric conductivity. Among them, inductance and capacitance are used here to explain the phenomena of this technique.

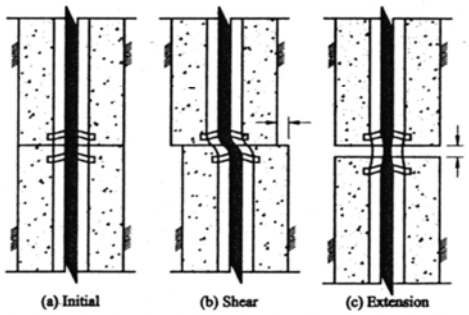

FIG. 1. Type of Block Movement and Change of Fixed Cable Geometries

[1]Assoc. Prof., Dept. of Civ. Engrg., Nat. Chung-Hsing Univ., 250 Kuo-Kwan Rd., Taichung, Taiwan, R.O.C. (corresponding author). E-mail: MBSU@dragon.nchu.edu.tw

[2]PhD Candidate, Dept. of Civ. Engrg., Nat. Chung-Hsing Univ., 250 Kuo-Kwan Rd., Taichung, Taiwan, R.O.C.

Note. Editor-in-Chief: Jeff R. Wright. Discussion open until November 1, 2000. To extend the closing date one month, a written request must be filed with the ASCE Manager of Journals. The manuscript for this paper was submitted for review and possible publication on July 8, 1998. This paper is part of the ***Journal of Infrastructure Systems***, Vol. 6, No. 2, June, 2000. ©ASCE, ISSN 1076-0342/00/0002-0067–0072/$8.00 + $.50 per page. Paper No. 18745.

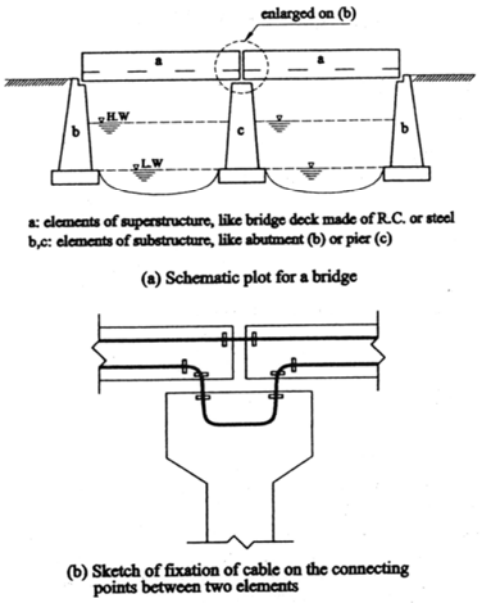

FIG. 2. Monitoring System for Relative Movement between Bridge Deck and Deck Joint or Bridge Bearing Point

Time domain analysis of wave motion is accomplished by looking at the motion of transverse electromagnetic waves. This is the simplest mode of electromagnetic wave field and is restricted to the plane normal to the wave propagation direction. By assuming the coaxial cable to be a lossless line, that is, with resistance and dielectric conductivity neglected, the governing equation of wave transmission in the system can be represented as

$$\partial^2 V/\partial x^2 = LC\partial^2 V/\partial t^2 \tag{1}$$

where L = inductance (henry); C = capacitance (farad); and $(L/C)^{1/2} = Z$ is called the characteristic impedance of the cable and is measured in ohms.

The above equation can be recognized as the basic wave equation for voltage pulse V as a function of distance x and time t. The magnitudes of L (inductance) and C (capacitance) for a coaxial cable are both functions of geometry between inner and outer conductors. By assuming the wave equation governs the behavior of the system, the reflected electrical signal can be analyzed in the time domain in a fashion similar to that for reflected seismic waves.

TYPE OF VOLTAGE REFLECTIONS

Coaxial cable deformation produce discontinuities that can be divided into two categories: a change in characteristic impedance Z_0 (type I), or a change in reactive lumped circuit elements (type II) (Dowding et al. 1988). Either type produces a reflected voltage pulse. Travel time between initiation and reflection of the pulse is converted to distance by specifying a propagation velocity, while the slope and amplitude of the reflection can be related to specific changes in cable properties. Since individual discontinuities are separated in space, they are also separated in time and thus can be analyzed separately. This relation between location and travel time forms the basis of TDR.

Cable Extension

When a metallic cable is deformed in tension, its diameter decreases as necking occurs. A decreased cross-sectional area

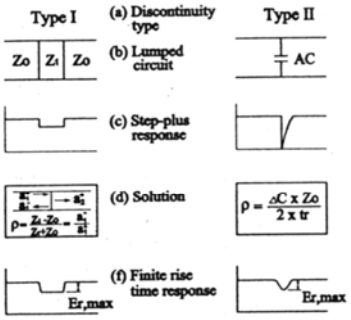

FIG. 3. Type of Reflected Signal and Idealization for Analysis (Dowding et al. 1989)

creates a new characteristic impedance, Z_1, different from the original, Z_0. At the interface, the reflection coefficient, ρ, can be defined in terms of characteristic impedance (type I), as shown in Fig. 3.

$$\rho = (Z_1 - Z_0)/(Z_1 + Z_0) \tag{2}$$

where Z_1 = new characteristic impedance of the cable; and Z_0 = original characteristic impedance of the cable.

Cable Shear

When a cable is deformed by shearing, the deformation is localized and the change in impedance can be modeled by adding an equivalent capacitance to the lumped circuit system. Then the reflection coefficient, ρ, cannot be expressed simply in terms of impedance, but must be idealized by a localized change in capacitance.

For the ideal shunted capacitance case, the reflection coefficient, ρ, can be approximated by

$$\rho = \Delta C \cdot Z_0/2 \cdot t_r \tag{3}$$

where ΔC = equivalent shunted capacitance; Z_0 = characteristic impedance of the cable; and t_r = rise time.

MULTIPLE REFLECTION

In the proposed setup for infrastructure integrity monitoring, deformations of joints at different locations are monitored simultaneously along one cable. This means that more than one signal is to be picked up at the same time. The capability to watch and distinguish between these changes is needed. The reslution of a TDR system in signal change is a few centimeters and depends on the system's risetime (Pierce et al. 1994), which is good enough for current application. Risetime of the pulse may change when it passes cable discontinuity. Su and Chen (1998), was provided a viable technique for analyzing multiple reflections, examine the phenomenon.

In a practical TDR measurement, the reflection risetime is finite and the measurement is thus limited in bandwidth. Typical circuit discontinuities along a transmission line have time constants much faster than the input pulse risetime, thus changing the ideal response to an impulse response. This is shown in Fig. 3, and the equivalent capacitance is calculated using the following equation:

$$C = \left| \frac{Z}{m \cdot Z_0} \right| \times [E_{r,\max}] \tag{4}$$

where m is the maximum slope of the voltage wave versus time and is controlled by the risetime of the incident waveform.

$$m = \left.\frac{dE_i}{dt}\right|_{\max} \text{ in } mV/s \tag{5}$$

Since capacitance is proportional to the reflection coefficient magnitude, $E_{r,\max}$ in (4), it will appear to be changed if the incident waveform's risetime (or m) is different.

Multiple discontinuities on a transmission line create effects that complicate TDR analysis. If the cable of interest is composed of several sections, each with its own distinct characteristic impedance, a part of the incident signal is reflected at each of these impedance discontinuities.

Also, a pulse is attenuated as it passes a discontinuity, and the waveform slope, m, becomes smaller. A discontinuity along a cable will attenuate the incident pulse and increase the risetime.

In order to overcome the problem caused by the effect of variation in pulse risetime, an integration approach is proposed herein to analyze reflections. The method, shown in Fig. 4, involves integrating the reflection over time

$$A = \int_{t_1}^{t_2} V(t)\, dt \tag{6}$$

where t_1 is the starting point of a TDR reflection that returns to its reference level at time t_2. The quantity A can be seen as the area of the increased voltage between t_1 and t_2. The magnitude of this area is proportional to the magnitude of the added equivalent capacitance.

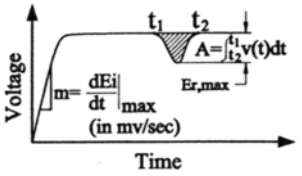

FIG. 4. Capacitance Calculated as Integration of Voltage Drop Over Time

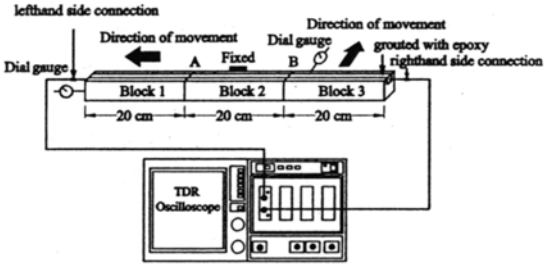

FIG. 5. Test Setup and Sample Dimensions

VALIDATION TEST

In order to show the applicability of multiple points monitoring at the same time, a validation test was performed. A semirigid coaxial cable is grouted into blocks using epoxy, and the blocks are arranged as shown in Fig. 5. Different amounts of relative movement between blocks are applied, and returned signatures are then recorded on the TDR oscilloscope. The purpose of this testing setup was twofold: (1) to show the different effects of joint deformation for shear and for extension, and (2) to test the resolution and effect of multiple discontinuities on the signature. The effect of multiple reflection is tested by taking signatures from different directions. When

TABLE 1. Complete Lists of Test Results

Position (1)	Measurement (2)	Deformation Type: Shear deformation at point B (mm) (3)	Deformation Type: Extension deformation at point A (mm) (4)	Area ($m\rho$-ps): Connection at left-hand side (5)	Area ($m\rho$-ps): Connection at right-hand side (6)	Area ($m\rho$-ps): Difference (%) (7)	$E_{r,\max}(m\rho)$: Connection at left-hand side (8)	$E_{r,\max}(m\rho)$: Connection at right-hand side (9)	$E_{r,\max}(m\rho)$: Difference (%) (10)
A	a	1	1	475.00	482.50	1.58	8.62	8.57	0.60
	b	1	2	1,068.75	1,040.00	2.69	11.05	10.56	4.45
	c	1	3	1,504.38	1,508.75	0.29	12.37	11.52	6.85
	d	1	4	1,845.00	1,820.63	1.32	11.77	13.29	12.97
	e	1	5	2,305.00	2,291.87	0.57	13.23	12.05	8.87
	f	1	6	2,743.75	2,681.25	2.28	13.23	12.05	8.88
	g	1	7	2,963.75	2,960.00	0.13	12.05	11.38	5.54
B	a′	1	7	285.83	281.44	1.56	9.36	11.34	17.46
	b′	2	7	667.68	669.57	0.28	21.42	22.20	3.51
	c′	3	7	1,146.97	1,140.34	0.58	32.56	41.14	20.86

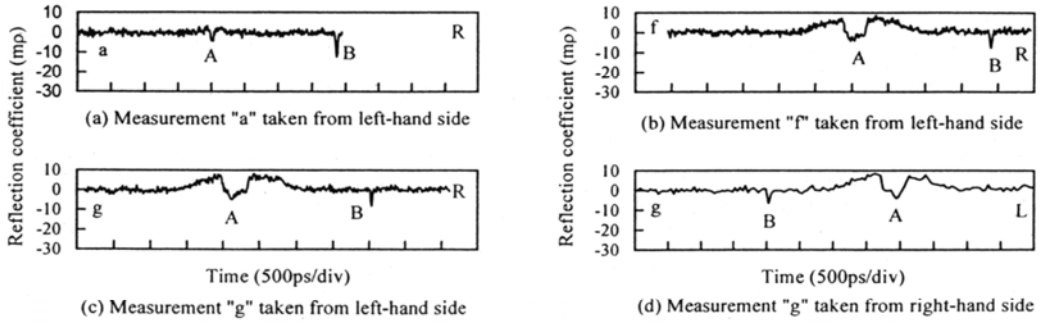

FIG. 6. Recorded Waveforms for Extension at Point A

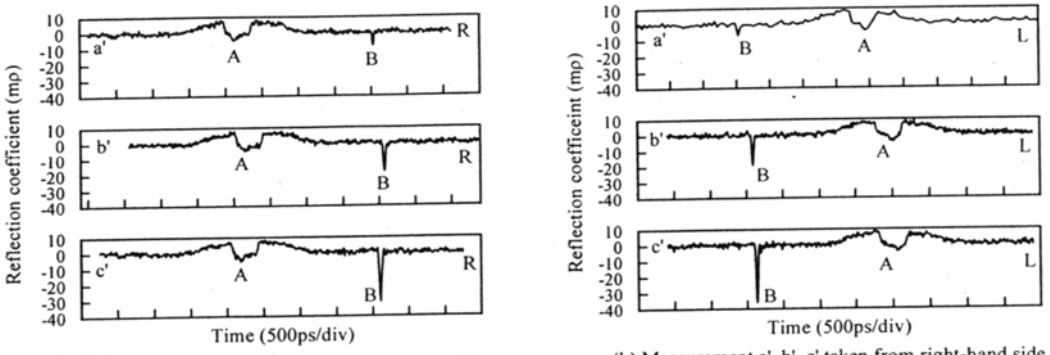

(a) Measurement a', b', c' taken from left-hand side

(b) Measurement a', b', c' taken from right-hand side

FIG. 7. Recorded Waveforms for Shearing at Point B

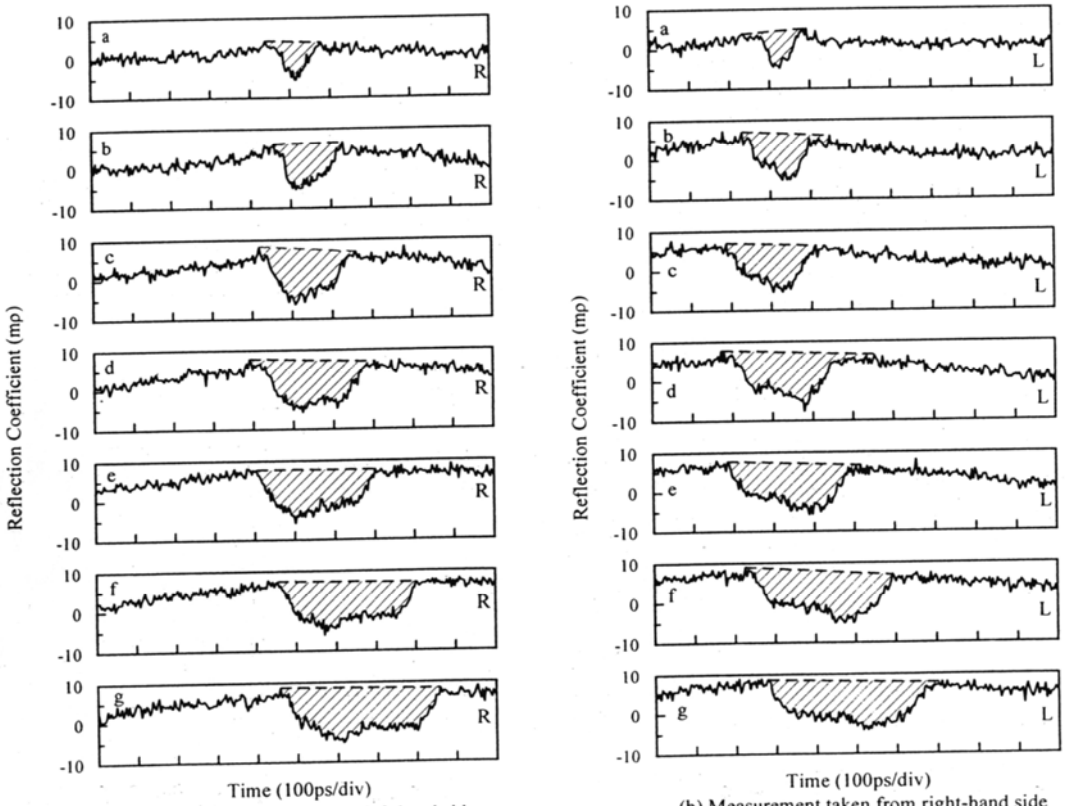

(a) Measurement taken from left-hand side

(b) Measurement taken from right-hand side

FIG. 8. Enlarged Waveforms of Each Measurement Taken for Extension at Point A

the reflected waveform is taken from the left-hand side, as shown in Fig. 5, the A discontinuity is encountered first. The waveform then passes B. When the waveform passes the A discontinuity, the risetime drops before it goes into B. When the reflected waveform is taken from right-hand side, the sequence is reversed. Test results for discontinuity points A and B are summarized in Table 1. In the test setup, block 1 is designed to be pulled away from block 2, which is fixed. Block 3 is designed to perform a shearing test by being moved laterally relative to block 2. First, block 3 is pushed laterally by 1 mm, then block 1 is pulled and measurements are taken. Data for seven different magnitudes of deformations are recorded. After that, block 3 is pushed laterally and three measurements are taken. Magnitudes of signature change at each reflection point are given separately in maximum reflected coefficient and integrated area of reflected coefficient. Differences in its magnitude are given in the last column to provide the basis of comparison.

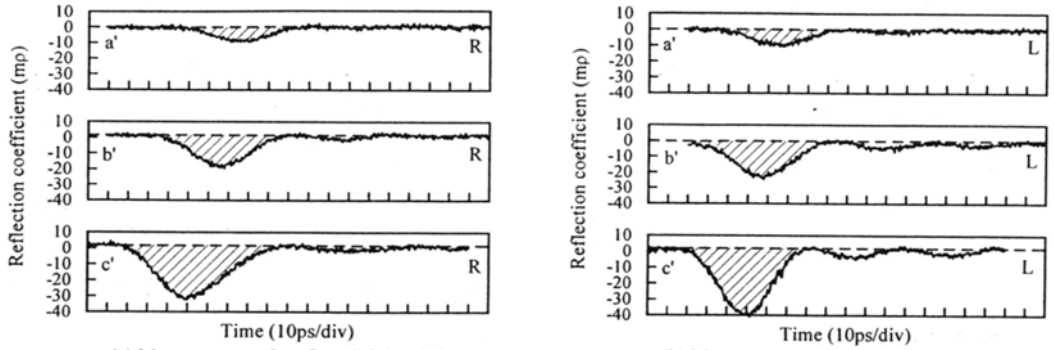

(a) Measurement taken from left-hand side

(b) Measurement taken from right-hand side

FIG. 9. Enlarged Waveforms of Each Measurement Taken for Shearing at Point B

DISCUSSION OF RESULTS

Locations of joints together with their movements are clearly shown in the waveform recorded as shown in Figs. 6 and 7. Fig. 6 shows waveforms for measurements taken after point B had 1 mm shear deformation and extension deformation is applied to point A. Figs. 6(a–c) are measurements taken from the same side of the cable; waveforms shown are all the same at point B, and the only difference is at point A. A larger magnitude of extension deformation generated a larger change of waveform. Records (c) and (d) are taken from different sides of the cable under the same situation. As can be seen, waveforms are reversed. Fig. 7 is waveforms for measurements a′, b′, and c′, which are taken to show signature change for shearing deformation at point B after 7 mm extension deformation is applied to point A. The three waveforms for each column stand for records taken from the same side of the cable. The only difference is the magnitude of change in the waveform on point B in order to show the effect of shearing. Records on (a) and (b) are all reversed.

In order to quantify the change of waveform due to relative movement of blocks, Figs. 8 and 9 were prepared using enlarged plots to show the details. In Fig. 8, columns (a) and (b) are used to represent records taken from different sides of the cable. Seven waveforms in each column are for different magnitudes of relative extension of blocks at point A. As can be seen, the voltage drops around the deformation point and increases with increasing extension deformation. As still can be seen from waveform between columns (a) and (b), the shape of the waveform is inverted. Fig. 9 shows the enlarged waveforms of measurement at point B for shear deformation between blocks. Different amounts of shearing deformation produce different magnitudes of waveform change. Joints on the sides of the 20 cm blocks are large enough for the waveform change to be seen clearly, and the magnitude of the reflected waveform is noticeable and should be treated with the procedures proposed in Su and Chen (1998).

The differences in measurements taken from different connection points are within 3% for all 10 measurements, but if the maximum reflected voltage is used, the differences could be as large as 20.86%. This result is plotted separately in Figs. 10(a) and (b) for measurements of integrated area and maximum reflected voltage. In both plots, measurements taken from the left-hand side are given as the x-axis and from the right-hand side as the y-axis. Fig. 10(a) shows a much better correlation, as almost all points are located on the slope equal to one line.

Figs. 11 and 12 are drawn to show individually the relationships between the integrated area of signature and the dial readings for extension and shear deformation. A linear plot is

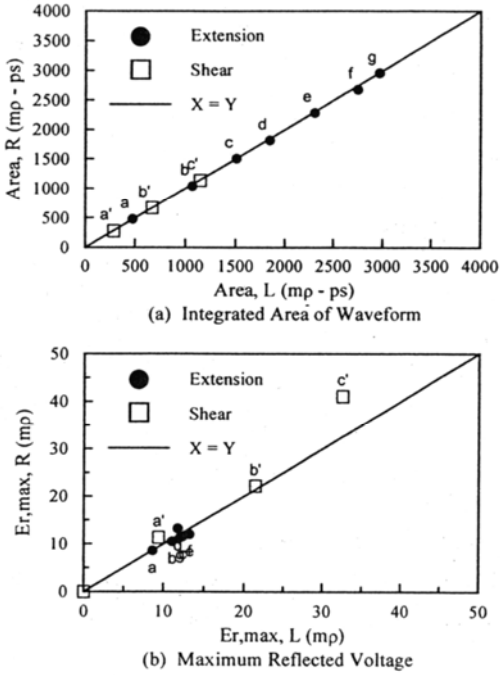

(a) Integrated Area of Waveform

(b) Maximum Reflected Voltage

FIG. 10. Comparisons between Data Taken from Different Connection Points

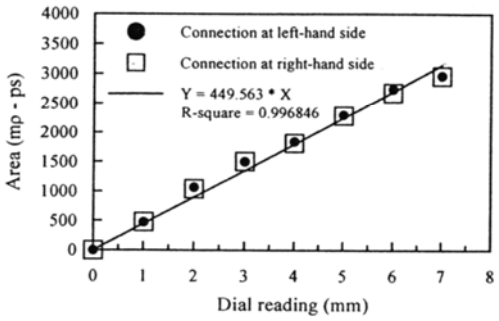

FIG. 11. Relationship between Integrated Area and Extension Movement of Block

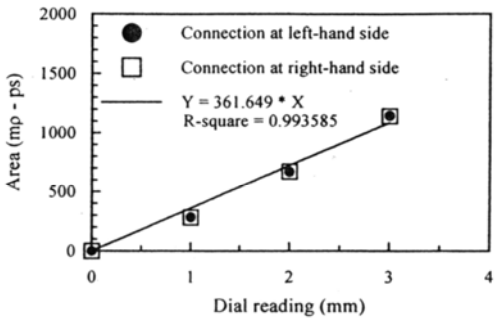

FIG. 12. Relationship between Integrated Area and Shear Movement of Block

given to show the applicability, which has an R-square value larger than 0.99. This regression relation can be used to quantify deformation based on the signature change.

The waveform did change after passing through cable deformation, that is, cable's impedance change. Risetime of the waveform and its reaction with the next interface changed. The area integration method did prove to be an acceptable analyzing method in multiple reflection situations, which makes possible the monitoring system for the integrity of infrastructure using only one coaxial cable.

CONCLUSION

The TDR technique can be applied to monitor the relative movement between elements of a structural system so as to assure its integrity or to provide a warning before large local failures. The coaxial cable can be fixed on both sides of a joint or grouted into elements, depending on the type of structure and field conditions. The cable then works like a multiple points relative movement sensor and waveform-transmitting medium. This technique is proven to be able to see multiple deformations simultaneously by using one cable and is easy to install as a smart monitoring tool for the integrity of a structural system.

APPENDIX I. REFERENCES

Cole, R. H. (1975). "Evaluation of dielectric behavior by time domain spectroscopy: 1. Dielectric response by real time analysis; 2. Complex permeability; 3. Precision difference methods." *J. Phys. Chem.*, 79(4), 1459–1474.

Dowding, C. H., and Huang, F.-C. (1994). "Early detection of rock movement with time domain reflectometry." *J. Geotech. Engrg.*, ASCE, 120(8), 1413–1427.

Dowding, C. H., Su, M. B., and O'Connor, K. M. (1989). "Measurement of rock mass deformation with grouted coaxial antenna cables." *Rock Mech. and Rock Engrg.*, Vol. 22, 1–23.

Dowding, C. H., Su, M. B., and O'Connor, K. M. (1988). "Principles of time domain reflectometry applied to measurement of rock mass deformation." *Int. J. Rock Mech. Min. Sci.*, 25(5), 287–297.

Lin, M. W., Abatan, A. O., and Danjaji, M. B. (1997). "Electrical time domain reflectometry sensing cables as distributed stress/strain sensors in smart material systems." *Proc., SPIE's 4th Annu. Symp. on Smart Struct. and Mat.*, International Society for Optical Engineering, Bellingham, Wash., Vol. 3024, 33–44.

Lin, M. W., Abatan, A. O., and Zhang, W. (1998). "Crack damage detection of structures using electrical time domain reflectometry (ETDR) sensors." *Proc., 5th Annu. Symp. on Smart Struct. and Mat.*, SPIE, San Diego, CA, Vol. 3325, 173–180.

Moffit, L. R. (1964). "Time domain reflectometry—Theory and applications." *Engrg. Des. News*, 38–44.

Pierce, C. E., Bilaine, C., Huang, F.-C., and Dowding, C. H. (1994). "Effects of multiple crimps and cable length on reflection signatures from long cables." *Proc., Symp. on Time Domain Reflectometry in Envir., Infrastructure, and Min. Applications, Spec. Publ. SP 19-94, NTIS PB95-105789*, U.S. Bureau of Mines, Washington, D.C., 540–554.

Su, M. B. (1990). "Fracture monitoring within concrete structure by time domain reflectometry." *Engrg. Fracture Mech.*, Vol. 35, 313–320.

Su, M. B., and Chen, Y. J. (1998). "Multiple reflection of time domain reflectometry." *Experimental Techniques*, 22(1), 26–29.

Topp, G. C., Davis, J. C., and Annan, A. P. (1980). "Electromagnetic determination of soil water content: Measurements in coaxial transmission lines." *Water Resour. Res.*, 16(3), 574–582.

APPENDIX II. NOTATION

The following symbols are used in this paper:

C = capacitance;
E_i = magnitude of voltage of incident wave;
$E_{r,\max}$ = maximum of voltage of reflected wave;
L = inductance;
m = maximum slope of voltage wave in time;
t = time;
t_r = rise time;
t_1 = time of reflected wave start to rise;
t_2 = time of reflected voltage return to normal;
V = voltage pulse as function of distance and time;
X = distance;
Z = impedance;
Z_0 = cable characteristic impedance;
Z_t = impedance of new section;
ΔC = magnitude of equivalent shunted capacitance; and
ρ = reflection coefficient.